Int. J. Sci. R. Tech., 2026 3(7)
A Multidisciplinary peer-reviewed Journal
www.ijsrtjournal.com [ISSN: 2394-7063]

Original Article

Eco-Conscious Synthesis Of Molybdenum Oxide (MoO_3) Nanoparticles Using *Aloe Barbadensis* Extract And Their Structural And Morphological And Dielectric Studies

Munirajappa N. N.[1], Harisha[2], Daruka Prasad B.[3], R. B. Basavaraj[3], Somashekar M. N.[4], K. N. Sathish[5], Nagarathnamma R.[6], Rajeev Ramachandra Kolgi[7], Haleshappa R.[7]*

[1]Department of Physics, Government Science College, Nrupathunga University, Bengaluru-560001, Karnataka, India.
[2]Jnana Jyothi Educational Institutes Yelahanka Yelahanka New Town, Bengaluru-560064, Karnataka, India.
[3]Department of Physics, BMS Institute of Technology and Management, Bengaluru-560064, Karnataka, India.
[4]Department of Chemistry, HKE Society's Sree Veerendra Patil Degree College of Science, Arts & Commerce Sadashivanagar, Bengaluru- 560080, Karnataka, India.
[5]Department of Physics, Govt. First Grade College, Doddaballapura -561203, Karnataka, India.
[6]Department of Chemistry, Vemana Institute of Technology, #1, Mahayogi Vemana Road, 3rd Block, Kormangala, Bengaluru - 560 034, Karnataka, India.
[7]Department of Chemistry and Biochemistry, Government Science College, Nrupathunga University, Bangalore-560001, Karnataka, India.

ABSTRACT

The environmentally benign synthesis of *Aloe barbadensis* nanoparticles (NPs) in materials science and engineering research is gaining popularity, particularly for molybdenum-based nanomaterials. They have recently gained popularity in various industries due to their versatility. The current study focuses on manufacturing molybdenum oxide (MoO_3) nanoparticles utilizing *Aloe barbadensis* (Aloe vera) plant extract, Tetraethyl Orthosilicate, and Hexadecyl Trimethyl Ammonium Bromide. The prepared sample is annealed at temperatures, of 600^0C. These samples are examined using XRD, SEM, EDAX, TEM, UV, and dielectric studies. The XRD examination of MoO_3 NPs produced at 600^0C shows an orthorhombic structure with higher crystallinity. The sample is annealed at 700^0C for SEM, EDX and TEM investigation. EDX elemental analysis confirms the presence of MoO_3. The TEM picture interpretation reveals spherical particles ranging from 50 to 60nm, Of MoO_3 NPs.

Keywords: XRD, SEM, TEM, UV, Dielectric constant, green synthesis.

INTRODUCTION

Recently, many creative plans and processes have been devised to synthesize transition metal oxide nanoparticles [1]. Due to these materials' potential applications in various technological domains, intense research has been focused on them. Recently, the development of new materials has been the goal of basic and technological research due to their potential application in new devices [2]. Among these materials, there is great interest in synthesizing semiconductor oxides. The last three decades have seen a massive increase in the green production of nanoparticles (NPs). With a size range of 1 to 100 nanometers, the NPs have special characteristics that set them apart from bulk materials. These attributes consist of magnetic behavior, quantum effects, improved catalytic activity, size-dependent effects, optical features, and high surface reactivity [3]. These characteristics of NPs make them useful in various study domains, including materials science, electronics, medicine, agriculture, and energy. A more advantageous approach for biological applications is fine-tuning the band gap energy value

Relevant conflicts of interest/financial disclosures: The authors declare that the research was conducted in the absence of any commercial or financial relationships that could be construed as a potential conflict of interest.

by altering the NP production technique [4]. The application components of the NP field have been covered by the main research fields, including agriculture, medicine, and energy.

Molybdenum oxide (MoO_3) is a versatile transition metal oxide with distinctive chemical and physical properties, making it a crucial material for numerous industrial and technical applications. MoO_3 has exceptional catalytic, electrical, and optical properties owing to its high oxidation states. These qualities make it a necessary component in catalysts, sensors, batteries, and optoelectronic devices [5]. However, the practical application of molybdenum oxide is sometimes hampered by its low dispersibility and inclination to agglomerate, which might affect its efficiency and performance [6-8].

The combination of molybdenum oxide and surfactants provides new opportunities for maximizing its use in catalysis, electronic devices, and other sectors [9]. Surfactants not only enhance the physical qualities of MoO_3, but can also introduce other capabilities, such as increased selectivity in catalytic processes or enhanced electronic properties in semiconductors [10]. As a result, studying and developing molybdenum oxide with surfactants is a promising area of research that has the potential to improve the capabilities and efficiency of molybdenum oxide-based technologies [11]. This combination of molybdenum oxide and *Aloe barbadensis* gel enhances the physical and chemical properties of MoO_3 while also aligning with the emerging trend of sustainable and eco-friendly materials [12].

The investigation of this novel hybrid material offers a promising field of research, with potential advances in catalysis, electronics, and biological applications, demonstrating the enormous advantages of combining natural products with modern materials [13]. Innovative approaches and materials are being investigated. One such potential technique is the use of *Aloe barbadensis* gel as a natural surfactant and stabilizing agent. *Aloe barbadensis* gel, generated from the Aloe barbadensis plant, contains polysaccharides, vitamins, and minerals, which give it special features like biocompatibility, biodegradability, and non-toxicity. These properties make *Aloe barbadensis* gel an appealing green alternative to synthetic surfactants [14].Combining *Aloe barbadensis* gel and molybdenum oxide improves particle dispersibility and stability in different mediums, reducing agglomeration and preserving a large surface area [15].

Furthermore, the biocompatibility of *Aloe barbadensis* gel may open up new avenues for the use of molybdenum oxide in biomedical applications such as drug delivery systems and biosensors [16].Two surfactants that have shown promise for improving the characteristics of molybdenum oxide are tetraethyl orthosilicate (TEOS) and hexadecyl trimethyl ammonium bromide (CTAB). TEOS, a silicon-based chemical, serves as a precursor for silica production and is well-known for its ability to build a stable and homogeneous coating on particles [17]. This silica coating enhances the thermal stability and dispersion of MoO_3 particles. CTAB, a cationic surfactant, helps form micelles and disperse MoO_3 uniformly in aqueous solutions. CTAB can potentially provide other capabilities, such as increased surface charge and interaction with other chemicals [18]. The synergistic combination of TEOS and CTAB with molybdenum oxide is an innovative method to maximize its use in a variety of applications [19]. TEOS adds a protective silica layer to improve stability, whilst CTAB guarantees uniform dispersion and avoids agglomeration [20]. This dual-surfactant system enhances the physical properties of MoO_3 and enables new functions in catalysis, electronics, and other technologies. Exploring the combination of TEOS and CTAB with molybdenum oxide offers new possibilities for improving its performance and broadening its applications, demonstrating the potential of surfactant-assisted approaches in material science [20].

As far as we know, only a few studies have been conducted on the synthesis of nanosphere networks in the absence of surfactants, despite substantial studies on silica as a carrier. As a result, developing nano-network architectures without surfactants has significant scientific implications and extensive application opportunities. Wang, X. et al [21]. recently created network material without the use of surfactants, however, the nano disperser requires an expensive high-speed homogenizer, limiting its industrial use Kupikowska-Stobba, B et.al. In contrast, gas-liquid interface interactions could be used to guide the formation of various network-like nanostructures [22] Tetraethylorthosilicate (TEOS), also known as tetraethoxysilane, is a commonly used precursor in the synthesis of silica-based materials. TEOS is employed in classical melting gels processes to produce silica and other silicon-containing compounds. This method is pivotal in the creation of various nanostructured materials, including periodic mesoporous silica and organosilicas. Kaur, H. et.al,[23]

The goal of surface functionalization of hemp-derived cellulose using tetraethyl orthosilicate (TEOS) and polyvinylidene fluoride (PVDF)-based composite separator is to improve the cellulose's qualities for usage in cutting-edge applications, especially composite separators. Sirichaibhinyo et.al [24].Tham A et.al highlights the efficacy of LP-PLA in tuning GO's structural and chemical properties while exploring its synergy with silica-based precursors like TEOS.[25]

2. Materials and Methods Synthesis of MoO3 (Molybdenum oxide)

Samples	Nomenclature	Ammonium heptamolybda tetetrahydrate (AHT)	Aloevera gel (plant extract	Surfactant-1	Surfactant-2
MoO_3	M1	2.5g	0	0	0
MoO_3	MA3	2.5g	15ml	0	0
MoO3	MAT3	2.5g	15ml	2.1ml TEOS (Tetraethyl ortho silicate	0
MoO3	MATC	`2.5g	15ml	2.1ml TEOS(tetraet hylortho silicate	2.19g CTAB (hexadecyl trimethyl ammonium bromide)

Table 1 The different weight percentages Ammonium Heptamolybda Tetetrahydrate (AHT), TEOS (Tetraethyl Orthosilicate) and CTAB (Hexadecyltrimethylammonium Bromide)

2.1 Preparation of Aloevera

The scientific name for Aloe vera is *Aloe barbadensis*, it belongs to the Liliaceae (Asphodelacease) family. The pulp inside the *Aloe barbadensis* leaves is removed by carefully lifting them, cleaning them well, and scraping them. The pulp is then completely crushed without the addition of any water. To remove the precipitate, the solution is filtered through pure muslin fabric. The precipitate is subsequently used to carry out the solution combustion operation.

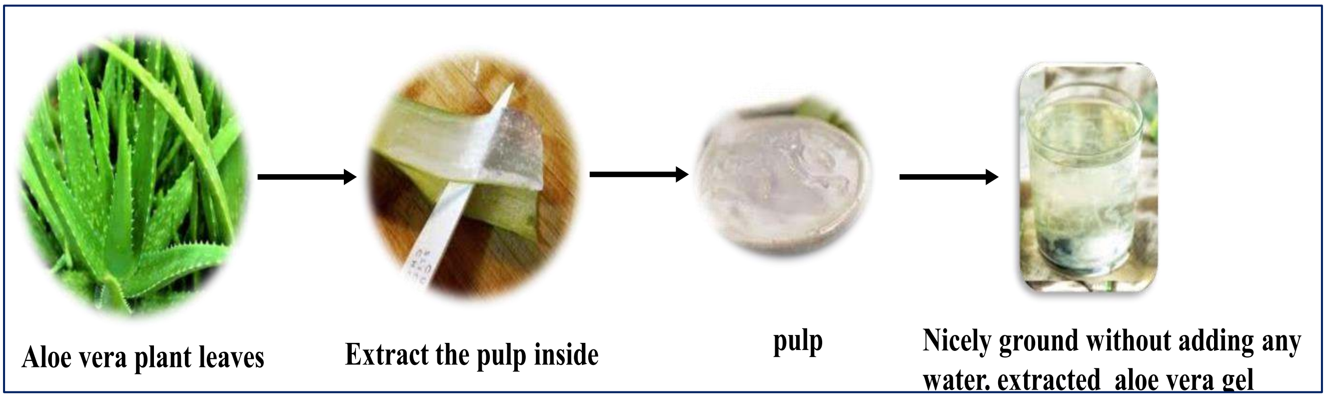

Figure -1 Schematic representation of Aloe barbadensis gel preparation.

2.2. Synthesis of MoO_3 NPs

A green combustion route was employed to synthesize MoO_3 NPs using the leaves of Aleo vera plant extract as a fuel. Initially, the plant leaves were dried in an autoclave and then pulverized to make a fine gel. *Aloe barbadensis* gel and molybdenum nitrate (analytical grade) were taken in 1:4 ratios in a silica crucible and swirled well using a magnetic stirrer for 5–10 min without water. The combination was placed in a pre-heated muffle furnace at 600° C and was allowed to react for a set duration, leaving a white powder with an extremely porous structure. Subsequently, the produced MoO_3 NPs were employed for structural and electrochemical research.

3. RESULT AND DISCUSSION

3.1 XRD (X-ray diffraction analysis)

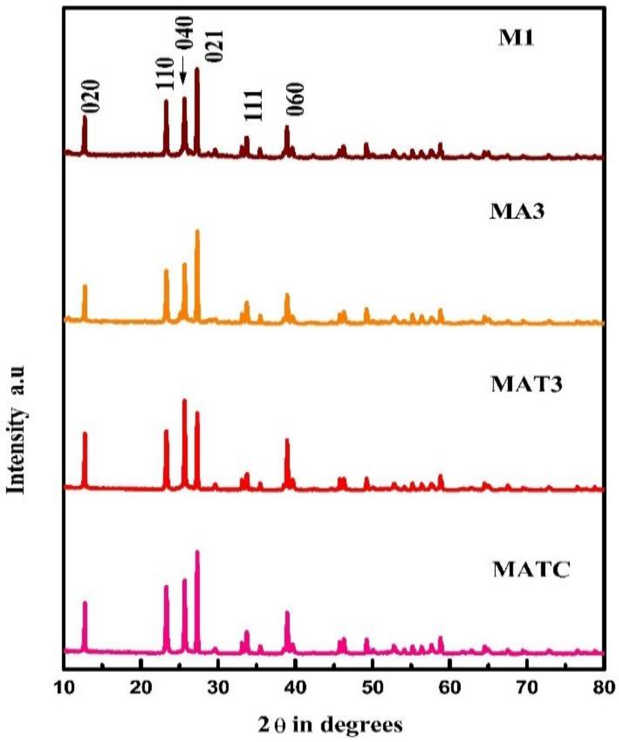

Figure 2a. XRD peaks of M1, MA3, MAT3, MATC nanoparticles

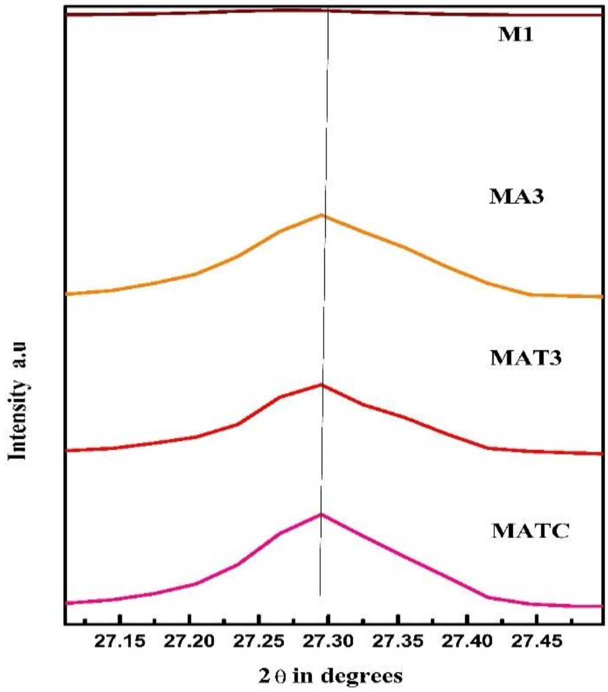

Figure 2b. XRD peaks shift at an angle 27.30° of M1, MA3, MAT3, MATC nanoparticles

Figure 2a depicts the X-ray diffraction (XRD) spectra of M1, MA3, MAT3, and MATC nanoparticles. The XRD spectrum shows pure with n sharp peaks, which indicates crystallite nature and orthorhombic structure. However, a diffuse broad peak ranging from 27° to 30° was observed which is broad peaks. The MoO_3 nanoparticles are in the spinel cubic structure and match with (JCPDS card no.96-900-9670, molybdenum oxide findings were also found to be consistent with the accepted references (JCPDS file no. 22-1012). The XRD pattern of MoO3 (**Figure 2**) shows that the main characteristic peak positions are slightly shifted toward the right side. the Pbnm is the space group and Orthorhombic structure with indexed planes near (020), (110), (040), (021), (111), and (060), respectively.

Using Scherrer's equation [26] (1), the average crystalline size was determined [27].

$$D_{hkl} = \frac{0.94\lambda}{\beta cos\theta} \quad (1)$$

Where,

λ = X-ray wavelength equal to 1.5406 A°

θ = Bragg diffraction angle,

β (radians) = full width at half maximum.

The average crystallite size of the samples was determined from the most conspicuous XRD line width of the (021) peak, and it was discovered that crystallite sizes typically fall between

Compound name	Crystal system	Crystallite size (nm)	Parameter (A^0)				R – factors			
			a	b	c	Cell volume ($A^{0\,3}$)	R_p	R_{wp}	GOF(χ^2)	Rex
M1	Orthorhombic	75	3.9	13.3	3.6	202	39.3	42	9	13
MA3		68	3.9	13.3	3.6	202	42.2	44	11	13
MAT3		55	3.9	13.3	3.6	202	50.5	47	6	17
MATC		61	3.9	13.3	3.6	203	49.4	45	4	20

Table 2. Rietveld refinement parameter from the PXRD data for MoO3

50 to 60 nm. The spectra showed a shift in peak position with the addition of surfactant TEOS and CTAB in the MoO3 NPs, attributed to a small modification in the structure. A similar trend was observed in several reported studies by different researchers [28].

3.2 SEM AND EDAX

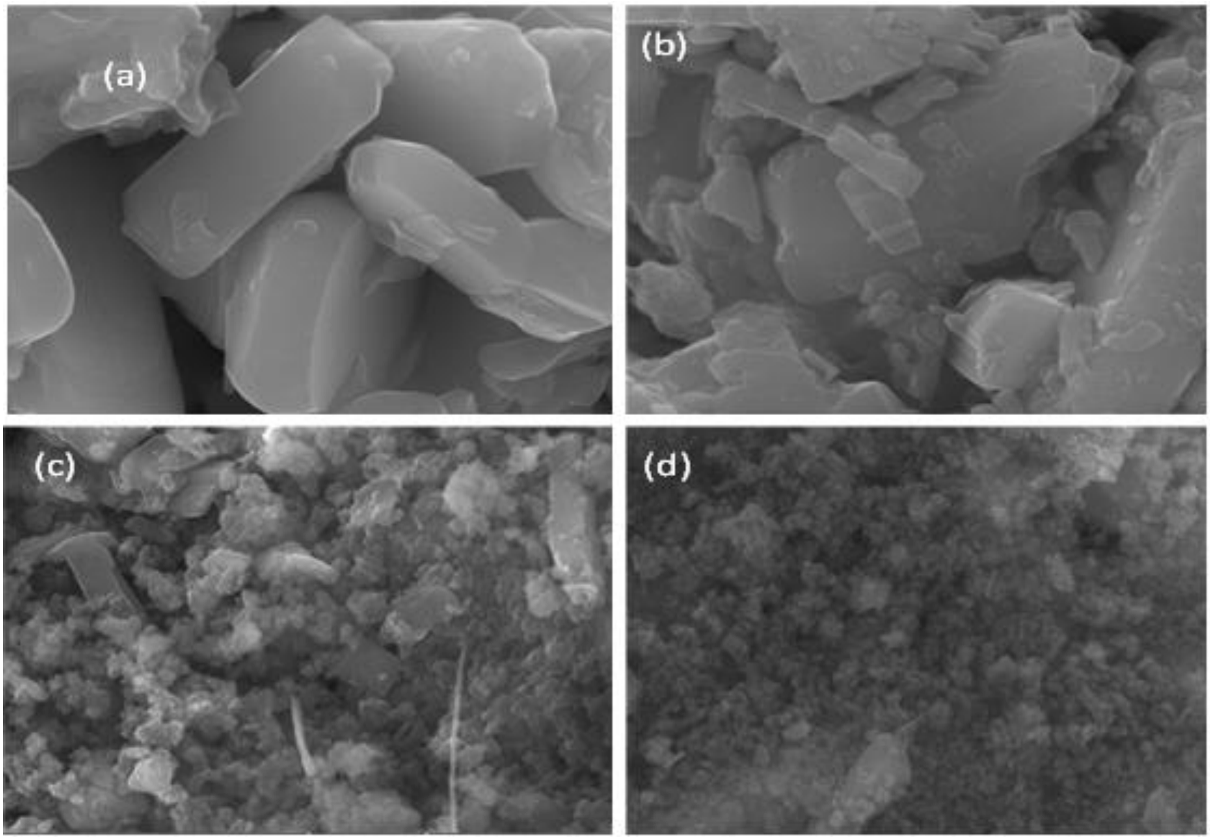

Figure 3. the SEM images M1, MA3, MAT3, MATC nanoparticle

creation of unique nanomaterial architectures or mesostructured. The SEM pictures in Figure 3 shows that the MoO_3 nanoparticles (NPs) have a homogenous surface, are granular, well-defined, and aggregated into cubic shapes. Nearly cubic shapes with an average particle size of 50–60 nm are revealed by a closer look at these fundamental structures. It is suggested that the nanoparticles have a crystalline character when the estimated crystallite size from X-ray diffraction analysis is compared with the observed nanoparticle morphology [28]

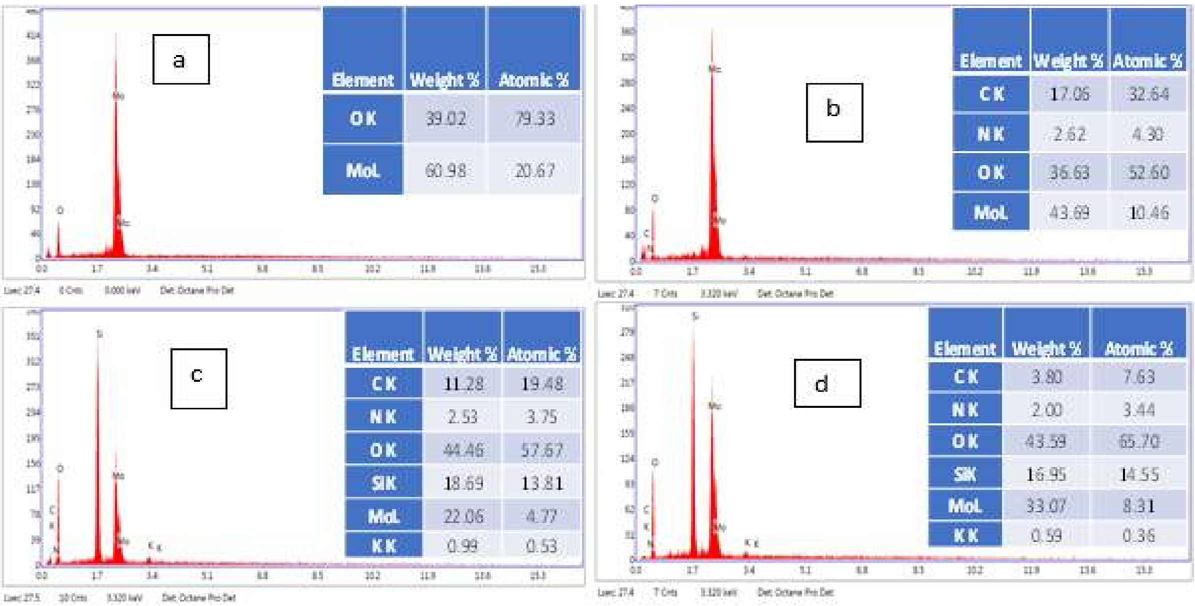

Figure 4: EDAX spectra (a)M1 (b)MA1 (c)MAT3, (d)MATC

The analysis technology known as energy-dispersive X-ray (EDX) spectroscopy is used to determine the chemical composition of a material. Energy-dispersive X-ray (EDX) analysis is employed to confirm the elemental assessment in the case of MoO3 nanoparticles. The findings are shown in Figure 4. Mo and O were found in the prepared samples of (a), (b), (c), and (d) MoO3 NPs, demonstrating their high purity. The EDX results and X-ray diffraction (XRD) data were extremely similar [29].

4. TEM (transmission electron microscope)

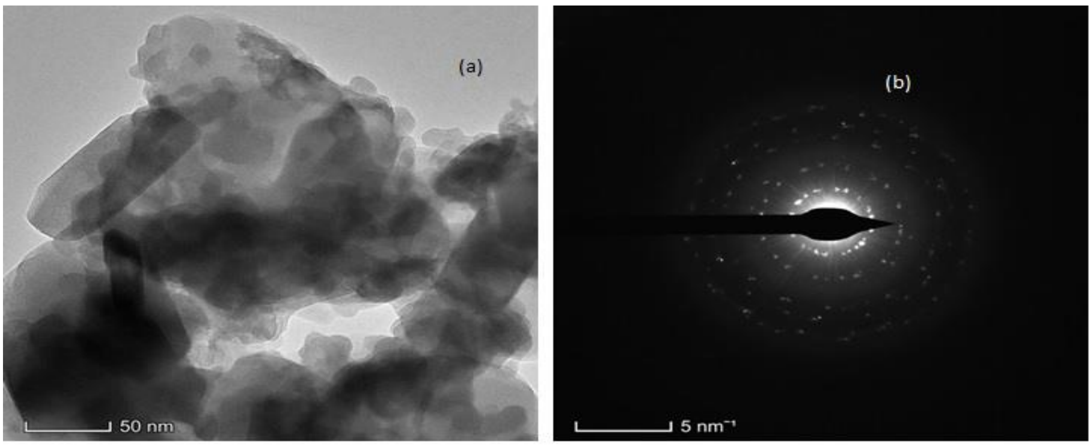

Figure 5: TEM images (a) HR- TEM of MA1 and SEAD pattern of MA1

High-resolution pictures were obtained using a Transmission Electron Microscope (TEM). Figure -5 shows the samples' detailed structures. The photos confirm the spherical shape with apparent agglomerations. Patchy circular rings with no diffraction spots and secondary phase rings suggest an Orthorhombic crystalline structure [30]. TEOS and CTAB are combined during the synthesis process and analyzed by TEM, the morphology, size, and structural properties of the nanoparticles or mesoporous materials can be thoroughly examined, providing exact control over the architecture of the nanomaterial.

5. Optical properties

5.1 Energy Bandgap analysis

Figures 6, display the UV-visible absorption spectra of compounds, The peak observed at 400 nm is attributed to the band transition originating from Mo-O bonds. Wood and Tauc introduced a method (equation 5) for calculating the energy gap (E_g). The equation is defined as follows:

$$\alpha h\gamma = A\,(h\gamma - E_g)^n \quad \ldots\ldots\ldots\ldots\ldots\ldots\ldots\ldots \quad (5)$$

In this equation, E_g represents the band gap energy, α denotes the absorption coefficient, A is a proportionality constant that varies based on the specific transition, hγ represents the photon energy, and the value of n depends on the nature of the transition (n = direct allowed, n = 1/2 in direct allowed, 3/2 forbidden direct, or n = 3 forbidden indirect electronic transitions).

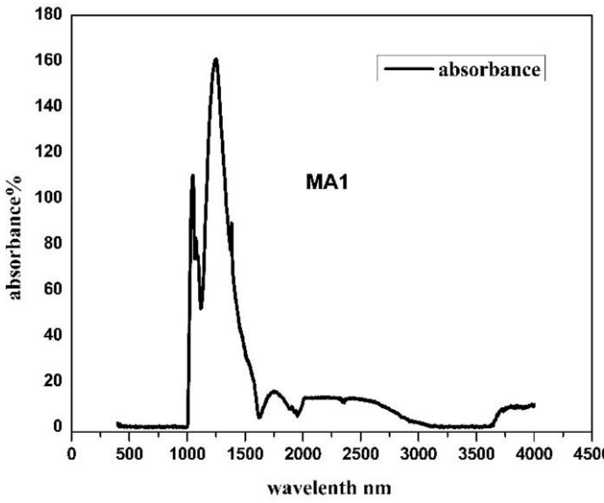

Figure 6. UV-visible absorption spectra of Nanoparticles.

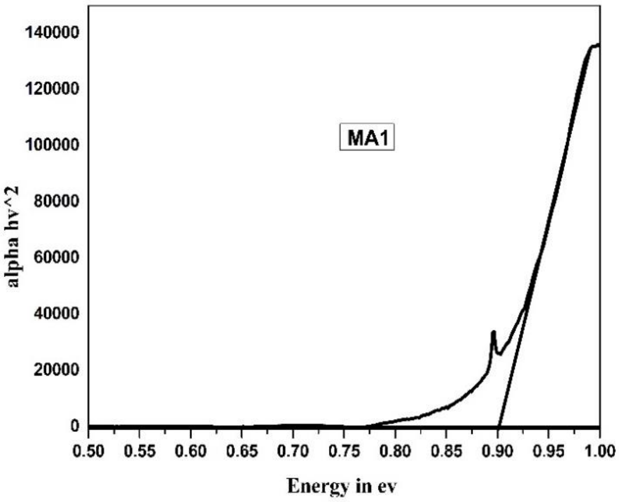

Figure 7. Energy bandgap of nanoparticles

Figure 6 displays the UV-visible absorption spectra of the produced samples. Extrapolating the plot on the X-axis provides a decent approximation of the bandgap. Figure 7 shows that the predicted bandgap values for the produced compounds range between 0.9. Notably, the energy band gap fluctuates with the concentration of Mo ions substituted for individual atoms in MoO3 nanoparticles. These variations in band gap values are linked to changes in the structural order-disorder within the lattice, causing shifts in the intermediate energy levels.[31, 32].

6. Dielectric constant

The dielectric characteristics of all the samples were investigated at room temperature using an impedance analyzer (Wayne Kerr 6500B). The fluctuation of the dielectric constant with frequency is shown in Figure and demonstrates inverse proportionality a characteristic behavior of MoO3. This phenomenon of increased dielectric constant with a decrease in frequency increases following Koops and can be attributed to conducting grains with insulating grain boundaries. It is well explained by space charge polarization, where the non-ferroelectric regions surround the ferroelectric regions—figure 8. MoO3 nanoparticles have real and imaginary dielectric constants. Figure 9 depicts the variation of dielectric loss concerning frequency [33-37].

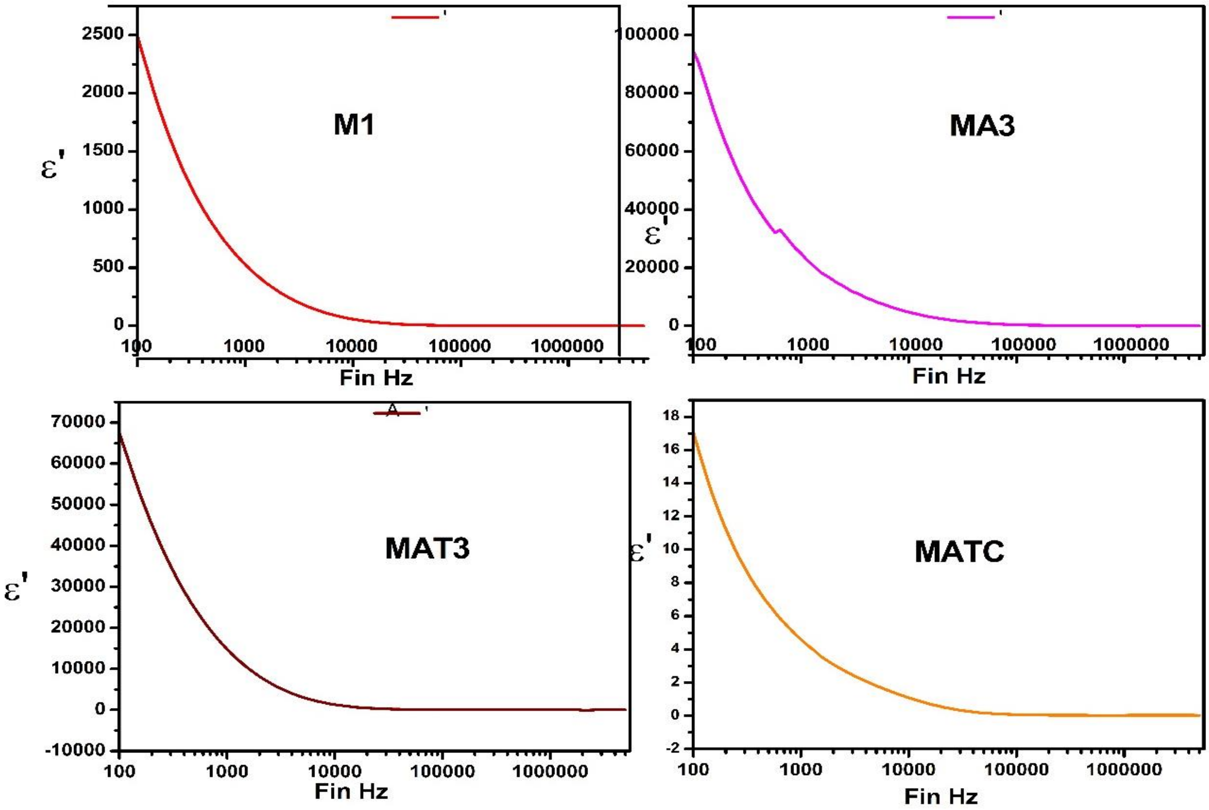

Figure 8: the real dielectric constant of M1, MA1, MAT3 MATC nanoparticles

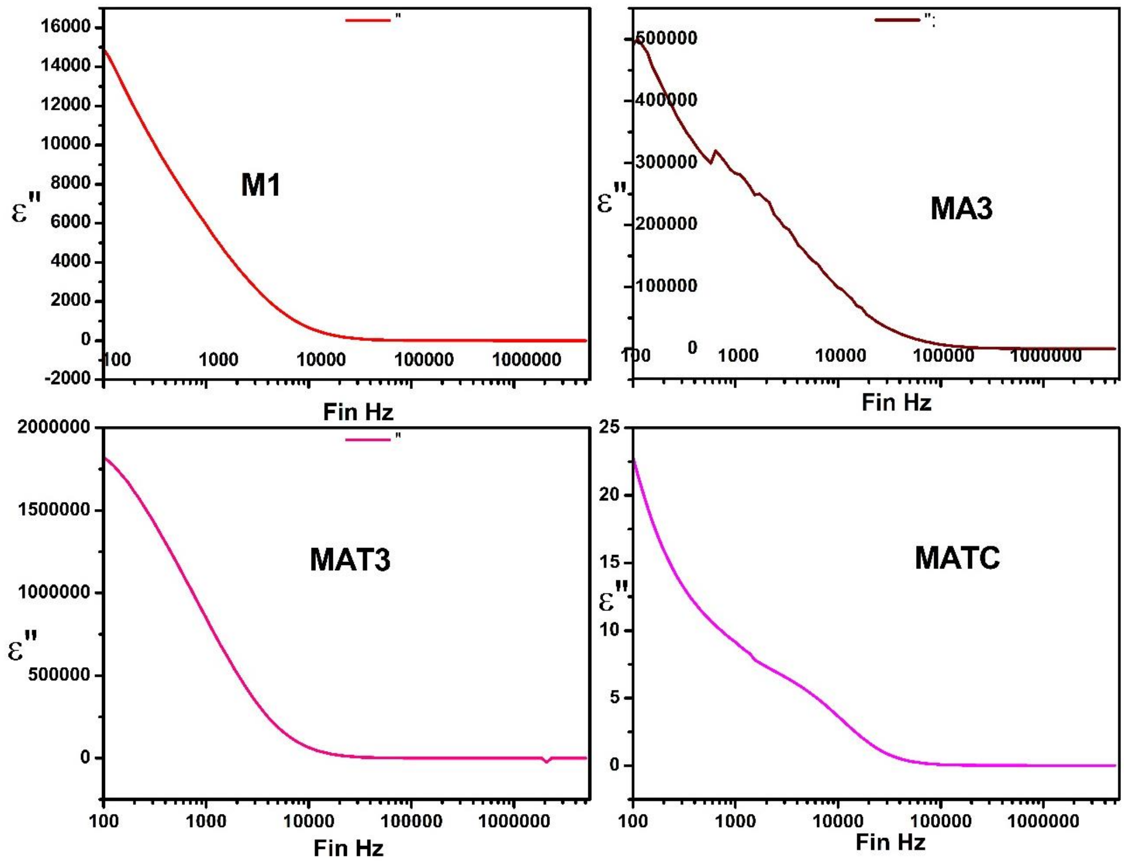

Figure 9: the imaginary dielectric constant of M1, MA1, MAT3 MATC nanoparticles

CONCLUSION

The primary goal for this study is to investigate the structural, morphological, UV, and dielectric properties of MoO3 nanoparticles generated using a novel green synthesis method (*Aloe barbadensis* gel extract) of use surfactants TEOS and CTAB. The XRD revealed that the compounds synthesized have the Pbnm is the space group and Orthorhombic structure. The substitution surfactants TEOS and CTAB is responsible for the increased crystalline size, and the sample size between 50 and 60 nm SEM and TEM were used to determine the surface morphology, and the study revealed with 50 to 60 nm crystal size. EDAX examination shows purity and homogeneity, whereas TEM reveals the existence of secondary phase rings with Orthorhombic structures. The band gap is 0.9 eV for u-v studies. Research indicates that CTAB has a higher ε' value, making it a promising material for electronic devices due to its dielectric constant and usage in electrical equipment.

REFERENCES

1. Maduraiveeran, G., Sasidharan, M., & Jin, W. (2019). Earth-abundant transition metal and metal oxide nanomaterials: Synthesis and electrochemical applications. Progress in Materials Science, 106, 100574.
2. Nicole, L., Rozes, L., & Sanchez, C. (2010). Integrative approaches to hybrid multifunctional materials: from multidisciplinary research to applied technologies.
3. Khan, I., Saeed, K., & Khan, I. (2019). Nanoparticles: Properties, applications and toxicities. Arabian journal of chemistry, 12(7), 908-931.
4. Salem, S. S., Hammad, E. N., Mohamed, A. A., & El-Dougdoug, W. (2022). A comprehensive review of nanomaterials: Types, synthesis, characterization, and applications. Biointerface Res. Appl. Chem, 13(1), 41.
5. Dalle Feste, P., Crisci, M., Barbon, F., Tajoli, F., Salerno, M., Drago, F., ... & Lamberti, F. (2021). Work function tuning in hydrothermally synthesized vanadium-doped MoO3 and Co3O4 mesostructures for energy conversion devices. Applied Sciences, 11(5), 2016.
6. Khusayfan, N. M., & Khanfar, H. K. (2020). Design and Characterization of MoO 3/Mg/MoO 3 Interfaces. IEEE Transactions on Electron Devices, 67(10), 4354-4359.
7. Hassel, A. W. (2020). Production and evaluation of iridium oxide-based pH sensors.
8. Bhandari, B. (2022). ROLE OF TEMPERATURE ON RAMAN SPECTROSCOPY OF MOS_2 MONOLAYER SYNTHESIZED BY CHEMICAL VAPOUR DEPOSITION (CVD).
9. Ali, S. A., & Ahmad, T. (2022). Chemical strategies in molybdenum-based chalcogenides nanostructures for photocatalysis. International Journal of Hydrogen Energy, 47(68), 29255-29283.
10. Dalle Feste, P., Crisci, M., Barbon, F., Tajoli, F., Salerno, M., Drago, F., ... & Lamberti, F. (2021). Work function tuning in hydrothermally synthesized vanadium-doped MoO3 and Co3O4 mesostructures for energy conversion devices. Applied Sciences, 11(5), 2016.
11. Xing, Y., Cai, Y., Cheng, J., & Xu, X. (2020). Applications of molybdenum oxide nanomaterials in the synergistic diagnosis and treatment of tumor. Applied Nanoscience, 10, 2069-2083.
12. Bhagya, K. R., Jyothi, K. R., Hegde, V. N., Prasad, B. D., Nagabhushana, H., Sharma, S. C., & Nagabhushana, N. M. (2021). Orange-red emitting praseodymium doped yttrium-molybdate nanophosphors for multifunctional applications. Journal of Science: Advanced Materials and Devices, 6(2), 234-244.
13. Park, W., Shin, H., Choi, B., Rhim, W. K., Na, K., & Han, D. K. (2020). Advanced hybrid nanomaterials for biomedical applications. Progress in Materials Science, 114, 100686.
14. Faria-Silva, A. C., Mota, A. L., Costa, A. M., Silva, A. M., Ascenso, A., Reis, C., ... & Simões, S. (2022). Application of natural raw materials for development of cosmetics through nanotechnology. In Nanotechnology for the Preparation of Cosmetics Using Plant-Based Extracts (pp. 157-201). Elsevier.
15. Mallakpour, S., & Sirous, F. (2020). Environmentally sustainable organo-modification of selected metal oxides and their hybrids: Characterization, properties, and utilizations. In Green Sustainable Process for

Chemical and Environmental Engineering and Science (pp. 351-377). Elsevier.

16. Jeevanandam, J., Vadanasundari, V., Pan, S., Barhoum, A., & Danquah, M. K. (2022). Bionanotechnology and Bionanomaterials: Emerging Applications, Market, and Commercialization. Bionanotechnology: Emerging Applications of Bionanomaterials, 3-44.
17. Mora-Rodríguez, S. E., Camacho-Ramírez, A., Cervantes-González, J., Vázquez, M. A., Cervantes-Jauregui, J. A., Feliciano, A., ... & Lagunas-Rivera, S. (2022). Organic dyes supported on silicon-based materials: synthesis and applications as photocatalysts. Organic Chemistry Frontiers, 9(10), 2856-2888.
18. Anucha, C. B., Altin, I., Bacaksiz, E., & Stathopoulos, V. N. (2022). Titanium dioxide (TiO_2)-based photocatalyst materials activity enhancement for contaminants of emerging concern (CECs) degradation: In the light of modification strategies. Chemical Engineering Journal Advances, 10, 100262.
19. Izzudin, N. M., Jalil, A. A., Ali, M. W., Aziz, F. F. A., Azami, M. S., Hassan, N. S., ... & Hassim, M. H. (2022). Promoting a well-dispersion of MoO3 nanoparticles on fibrous silica catalyst via one-pot synthesis for enhanced photoredox environmental pollutants efficiency. Chemosphere, 308, 136456.
20. Li, H., Chen, X., Shen, D., Wu, F., Pleixats, R., & Pan, J. (2021). Functionalized silica nanoparticles: classification, synthetic approaches and recent advances in adsorption applications. Nanoscale, 13(38), 15998-16016.
21. Wang, X., Li, H., Shan, C., & Pan, B. (2022). Construction of model platforms to probe the confinement effect of nanocomposite-enabled water treatment. Chemical Engineering Journal Advances, 9, 100229.
22. Kupikowska-Stobba, B., & Kasprzak, M. (2021). Fabrication of nanoparticles for bone regeneration: new insight into applications of nanoemulsion technology. Journal of Materials Chemistry B, 9(26), 5221-5244.
23. Kaur, H., Chaudhary, S., Kaur, H., Chaudhary, M., & Jena, K. C. (2021). Hydrolysis and condensation of tetraethyl orthosilicate at the air–aqueous interface: implications for silica nanoparticle formation. ACS applied nano materials, 5(1), 411-422.
24. Sirichaibhinyo, Thanakrit, Satita Thiangtham, Nagahiro Saito, and Sarute Ummartyotin. (2024)"Surface functionalization of cellulose derived from hemp by tetraethyl orthosilicate (TEOS) and poly vinylidene fluoride (PVDF)-based composite separator membrane for lithium-ion batteries (LIBs)." Results in Engineering 23 102807.
25. Tham A, Siah KX, Noor IM, Ghazali I, Tan ST, Tamchek N. (2024) Fabrication and structural modification of graphene oxide-tetraethyl orthosilicate solution via liquid-phase pulsed laser ablation. Journal of Laser Applications.Feb 1;36(1).
26. Sen, S. K., Barman, U. C., Manir, M. S., Mondal, P., Dutta, S., Paul, M., ... & Hakim, M. A. (2020). X-ray peak profile analysis of pure and Dy-doped α-MoO3 nanobelts using Debye-Scherrer, Williamson-Hall and Halder-Wagner methods. Advances in Natural Sciences: Nanoscience and Nanotechnology, 11(2), 025004.
27. Sen, S. K., Paul, T. C., Dutta, S., Hossain, M. N., & Mia, M. N. H. (2020). XRD peak profile and optical properties analysis of Ag-doped h-MoO 3 nanorods synthesized via hydrothermal method. Journal of Materials Science: Materials in Electronics, 31, 1768-1786.
28. Izzudin, N. M., Jalil, A. A., Ali, M. W., Aziz, F. F. A., Azami, M. S., Hassan, N. S., ... & Hassim, M. H. (2022). Promoting a well-dispersion of MoO3 nanoparticles on fibrous silica catalyst via one-pot synthesis for enhanced photoredox environmental pollutants efficiency. Chemosphere, 308, 136456.
29. Zaid, O. F., El-Said, W. A., Yousif, A. M., Galhoum, A. A., Elshehy, E. A., Ibrahim, I. A., & Guibal, E. (2020). Synthesis of microporous nano-composite (hollow spheres) for fast detection and removal of As (V) from contaminated water. Chemical Engineering Journal, 390, 124439.
30. Yang, G., Yang, H., Zhang, X., Feng, F., Ma, J., Qin, J., ... & Ma, J. (2020). Surfactant-free self-assembly to the synthesis of MoO3 nanoparticles on mesoporous SiO2 to form MoO3/SiO2 nanosphere networks with excellent oxidative

desulfurization catalytic performance. Journal of Hazardous Materials, 397, 122654.

31. Sharma, S., & Basu, S. (2021). Visible-light-driven efficient photocatalytic abatement of recalcitrant pollutants by centimeter-length MoO3/SiO2 monoliths with long service life. Applied Materials Today, 23, 101033.
32. Zaid, O. F., El-Said, W. A., Yousif, A. M., Galhoum, A. A., Elshehy, E. A., Ibrahim, I. A., & Guibal, E. (2020). Synthesis of microporous nano-composite (hollow spheres) for fast detection and removal of As (V) from contaminated water. Chemical Engineering Journal, 390, 124439.
33. Heidarnia, Z., Parvizi, R., Khoshsima, H., & Heidari, H. (2022). Distinct absorption transducing features of silica supported MoO3/PANI hybrid coated optical fiber towards Malathion monitoring in food samples. Sensors and Actuators B: Chemical, 371, 132501.
34. Kunchakara, S., Ratan, A., Dutt, M., Shah, J., Kotnala, R. K., & Singh, V. (2020). Impedimetric humidity sensing studies of Ag doped MCM-41 mesoporous silica coated on silver sputtered interdigitated electrodes. Journal of Physics and Chemistry of Solids, 145, 109531.
35. Holler, B. A., Crowley, K., Berger, M. H., & Gao, X. P. (2020). 2D semiconductor transistors with van der Waals oxide MoO3 as integrated high-κ gate dielectric. Advanced Electronic Materials, 6(10), 2000635.
36. Maitra J, Kumar K. Fabrication and characterization of poly (methyl methacrylate)-based nanocomposite films reinforced with plant-mediated copper oxide nanoparticles. Polymer Bulletin. 2026 Oct;83(10):545.
37. Kavyashree D, Hosur SB, Yashwanth HJ, Anusha NN, Naik MM, Sunitha DV, Shetty HD. Eco-friendly synthesis of $NiMoO_4$ nanoparticles for efficient photocatalytic dye degradation. Polyhedron. 2026 May 29:118225.

HOW TO CITE: Munirajappa N. N.[1], Harisha[2], Daruka Prasad B.[3], R. B. Basavaraj[3], Somashekar M. N.[4], K. N. Sathish[5], Nagarathnamma R.[6], Rajeev Ramachandra Kolgi[7], Haleshappa R.[7]*, Eco-Conscious Synthesis Of Molybdenum Oxide (MoO_3) Nanoparticles Using Aloe Barbadensis Extract And Their Structural And Morphological And Dielectric Studies, Int. J. Sci. R. Tech., 2026, 3 (7), 771-781. https://doi.org/10.5281/zenodo.21508815